Cancer Cell
Article

A TARBP2-Dependent miRNA Expression Profile Underlies Cancer Stem Cell Properties and Provides Candidate Therapeutic Reagents in Ewing Sarcoma

Claudio De Vito,[1,3] Nicolo Riggi,[1,3] Sandrine Cornaz,[1] Mario-Luca Suvà,[1] Karine Baumer,[1] Paolo Provero,[2] and Ivan Stamenkovic[1,*]
[1]Institute of Pathology, Centre Hospitalier Universitaire Vaudois, Faculty of Biology and Medicine, University of Lausanne, Lausanne, Switzerland
[2]Department of Genetics, Biology and Biochemistry, University of Torino, Torino, Italy
[3]These authors contributed equally to the work
*Correspondence: ivan.stamenkovic@chuv.ch
DOI 10.1016/j.ccr.2012.04.023

SUMMARY

We have recently demonstrated that human pediatric mesenchymal stem cells can be reprogrammed toward a Ewing sarcoma family tumor (ESFT) cancer stem cell (CSC) phenotype by mechanisms that implicate microRNAs (miRNAs). Here, we show that the miRNA profile of ESFT CSCs is shared by embryonic stem cells and CSCs from divergent tumor types. We also provide evidence that the miRNA profile of ESFT CSCs is the result of reversible disruption of TARBP2-dependent miRNA maturation. Restoration of TARBP2 activity and systemic delivery of synthetic forms of either of two of its targets, miRNA-143 or miRNA-145, inhibited ESFT CSC clonogenicity and tumor growth in vivo. Our observations suggest that CSC self-renewal and tumor maintenance may depend on deregulation of TARBP2-dependent miRNA expression.

INTRODUCTION

Cancer development is a multistep process that relies primarily on alterations in the form of mutation, deletion, or translocation of genes that control cell growth, proliferation, and survival. Mounting evidence suggests that, despite originating from a single transformed cell, a tumor may adopt a hierarchical cellular organization, the apex of which is occupied by poorly differentiated cells that acquire or retain at least a subset of stem cell properties, including the capacity for self-renewal and differentiation (Clarke et al., 2006; Clevers, 2011; Frank et al., 2010; Visvader, 2011). These cells, termed cancer stem cells (CSCs), have the ability to generate proliferating cell pools that repopulate tumors and to differentiate into nontumorigenic progeny that contributes to the phenotypic heterogeneity characteristic of most tumor types. CSCs have therefore been advocated to constitute the sustaining force of a tumor. This notion has led to the view that CSC-directed therapeutic approaches may provide an attractive alternative in malignancies that are resistant to conventional chemotherapy aimed at indiscriminate elimination of the tumor bulk (Frank et al., 2010).

Exactly how CSCs emerge remains unclear but possible mechanisms include transformation of primary stem cells or acquisition of stem cell properties by more differentiated cells as a result of transformation-associated genetic reprogramming (Liu et al., 2009; Marión et al., 2009). Subsequent maintenance of stem cell features may be ensured, in part, by the genetic alterations responsible for transformation itself and, in part, by posttranscriptional events, including regulation of gene expression by microRNAs (miRNAs).

miRNAs are noncoding transcripts capable of recognizing complementary sequences within the 3′ untranslated regions, introns, and even exons of a wide range of genes (Bartel, 2009). Human tumors display broad miRNA downregulation that appears to be responsible, at least in part, for their malignancy and stems from defects in their production, intracellular

Significance

Mechanisms that generate cancer stem cells (CSCs), which are believed to constitute the driving force of many malignancies, are poorly understood. We show that Ewing sarcoma family tumor (ESFT) CSCs emerge as a result of a defect in microRNA (miRNA) maturation stemming from reversible repression of the gene encoding TARBP2, a protein implicated in stabilizing the miRNA processing machinery. The resulting miRNA expression repertoire regulates networks of genes whose expression changes underlie ESFT pathogenesis. Reconstitution of TARBP2 function or expression of its target miRNAs blunts ESFT CSC tumor-forming capacity and offers an attractive therapeutic option for one of the most aggressive pediatric malignancies.

transport, and/or maturation (Kumar et al., 2007; Melo and Esteller, 2011; Ventura and Jacks, 2009). miRNA biogenesis is a multistep process initiated by RNA polymerase II-mediated transcription to generate a primary miRNA (pri-miRNA) (Newman and Hammond, 2010; Winter et al., 2009). Pri-miRNAs are processed by the multiprotein microprocessor complex that includes Drosha, an RNaseIII enzyme, and DGCR8, a double-stranded RNA-binding domain protein, to produce a ~70 nt precursor miRNAs (pre-miRNAs). Pre-miRNAs are exported from the nucleus to the cytoplasm by Exportin-5 by a Ran-GTP-dependent mechanism and are further processed by the multiprotein Dicer complex to generate mature 21–23 nt oligomers. The two miRNA strands are then separated, and one is loaded onto the RNA-induced silencing complex (RISC) by binding to an Argonaute (Ago) protein, whereas the carrier strand is degraded (Newman and Hammond, 2010; Winter et al., 2009). The miRNA guides RISC to its complementary sequences within target transcripts to silence their expression by either facilitating corresponding mRNA degradation or blocking its translation. Because complementary sequences to any given miRNA are found in numerous genes, a restricted number of miRNAs can regulate expression of large gene repertoires implicated in the control of key cell functions. Increasing evidence indicates miRNA involvement in stem cell generation, maintenance, and differentiation, as well as in tumor initiation and progression, consistent with the possibility that miRNAs may play a key role in CSC establishment. As active participants in the orchestration of tumor development, miRNAs may also provide potentially attractive therapeutic targets and/or reagents in cancer.

Work from our own laboratory has shown that miRNAs are implicated in the emergence of CSCs in Ewing sarcoma family tumors (ESFT), the second most common bone malignancy in children and young adults (Riggi et al., 2010). ESFTs are characterized by unique chromosomal translocations that give rise to fusion genes composed of EWS and one of several ets family members of transcription factors (Riggi et al., 2007). The most common fusion gene, *EWS-FLI1*, arises as a result of the chromosomal translocation t(11;22)(q24;q12) and is expressed in 85%–90% of ESFTs. The EWS-FLI-1 fusion protein is believed to provide the key oncogenic event in ESFT by inducing and repressing target genes that lead to transformation of permissive primary cells. Mesenchymal stem cells (MSCs) have been shown to provide permissiveness for EWS-FLI-1 expression and oncogenicity (Riggi et al., 2005, 2008) and are currently considered to be the most likely cell of origin of ESFT. Human pediatric MSCs (hpMSCs) transduced with EWS-FLI-1 (hpMSC$^{EWS\text{-}FLI\text{-}1}$) adopt a transcriptome that resembles that of ESFT more closely than any other primary or immortalized cell type tested (Riggi et al., 2010). Remarkably, expression of EWS-FLI-1 in hpMSCs cultured in serum-free conditions generates a subpopulation of cells that express the CD133 marker characteristic of CSCs in a variety of malignancies and in ESFT in particular (Suvà et al., 2009). These cells constitute no more than 5%–8% of the bulk hpMSC$^{EWS\text{-}FLI\text{-}1}$ population and display upregulation of the embryonic stem cell-associated genes *OCT4* and *NANOG* (Suvà et al., 2009) and repression of miRNA-145, a master regulator of ESC differentiation that acts by suppressing *OCT4*, *KLF4*, and *SOX2* expression (Xu et al., 2009). On the basis of these observations, we assessed miRNA implication in ESFT CSC development using reprogrammed hpMSC$^{EWS\text{-}FLI\text{-}1}$ cells, ESFT cell lines, and primary CSCs and addressed the mechanisms that underlie miRNA deregulation in CSCs.

RESULTS

The ESFT CSC Subpopulation Displays Repression of a Broad Range of miRNAs that Is Shared by the CD133$^+$ Fraction of hpMSC$^{EWS\text{-}FLI\text{-}1}$, Human Embryonic Stem Cells, Induced Pluripotent Stem Cells, and CSC from Diverse Carcinomas

To identify miRNAs that may be relevant to ESFT CSC generation and maintenance, we performed miRNA microarray expression profiling of the CD133$^+$ and CD133$^-$ subpopulations derived from primary ESFT, hpMSC$^{EWS\text{-}FLI\text{-}1}$, and the ESFT STA-ET-8.2 cell line. A total of four primary ESFT tumors were used, two of which (ESFT1 and 2) have been described previously (Suvà et al., 2009), whereas two others (ESFT3 and 4) were obtained more recently (Table S1 available online). All tumors displayed a poorly differentiated small round cell phenotype and harbored a subpopulation of CD133$^+$ cells ranging between 6.5% and 15.2%. Tumors 1 and 2 were used for initial miRNA profiling and qRT-PCR validation of miRNA expression, whereas tumors 3 and 4, whose CD133$^+$ subpopulations displayed features comparable to those of tumors 1 and 2 in terms of miRNA expression profiles, were used for all subsequent functional experiments. ESFT CD133$^+$ (corresponding to CSC) and CD133$^-$ cells were isolated from primary tumors, whereas CD133$^+$ and CD133$^-$ hpMSC$^{EWS\text{-}FLI\text{-}1}$ were generated by retrovirally mediated introduction of EWS-FLI-1 into hpMSCs grown in serum-free stem cell medium, as previously reported (Riggi et al., 2010). Expression profile analysis revealed broad miRNA repression in CD133$^+$ hpMSC$^{EWS\text{-}FLI\text{-}1}$ and ESFT cells, and cluster analysis showed that CD133$^+$ and CD133$^-$ cells derived from different primary ESFT cluster together, respectively (Figure 1A). The total number of miRNAs detected in ESFT samples 1 and 2 was 205 and 182, respectively. In CD133$^+$ cells of sample 1, 122 miRNAs (60%) were downregulated, whereas 29 (14%) were upregulated. In sample two, the corresponding numbers for CD133$^+$ cells were 102 (56%) and 4 (2%). Not surprisingly, a highly significant number of downregulated miRNAs was shared by CD133$^+$ ESFT and hpMSC$^{EWS\text{-}FLI1}$ cells (Figure 1B). miRNA repertoire distinction between CD133$^+$ and CD133$^-$ hpMSC$^{EWS\text{-}FLI\text{-}1}$ was found to resemble that between their respective primary ESFT CD133$^+$ and CD133$^-$ counterparts, as shown by the highly significant overlap between the lists of differentially expressed miRNAs (Figure 1B). Real-time PCR (qRT-PCR) assessment of the miRNA profile of CD133$^+$ and CD133$^-$ cell fractions derived from ESFT 1 and 2 and three distinct hpMSC$^{EWS\text{-}FLI\text{-}1}$ populations validated the microarray results, consistent with the notion that CD133$^+$ hpMSC$^{EWS\text{-}FLI\text{-}1}$ bear molecular resemblance to ESFT CSCs.

The above analysis was repeated using the ESFT cell line STA-ET-8.2, which has recently been suggested to mirror the CSC model (Jiang et al., 2010). However, microarray profiling of STA-ET-8.2-derived CD133$^+$ and CD133$^-$ subpopulations, as well as the corresponding qRT-PCR data validation, failed to show any difference in their miRNA repertoire, and no similarity

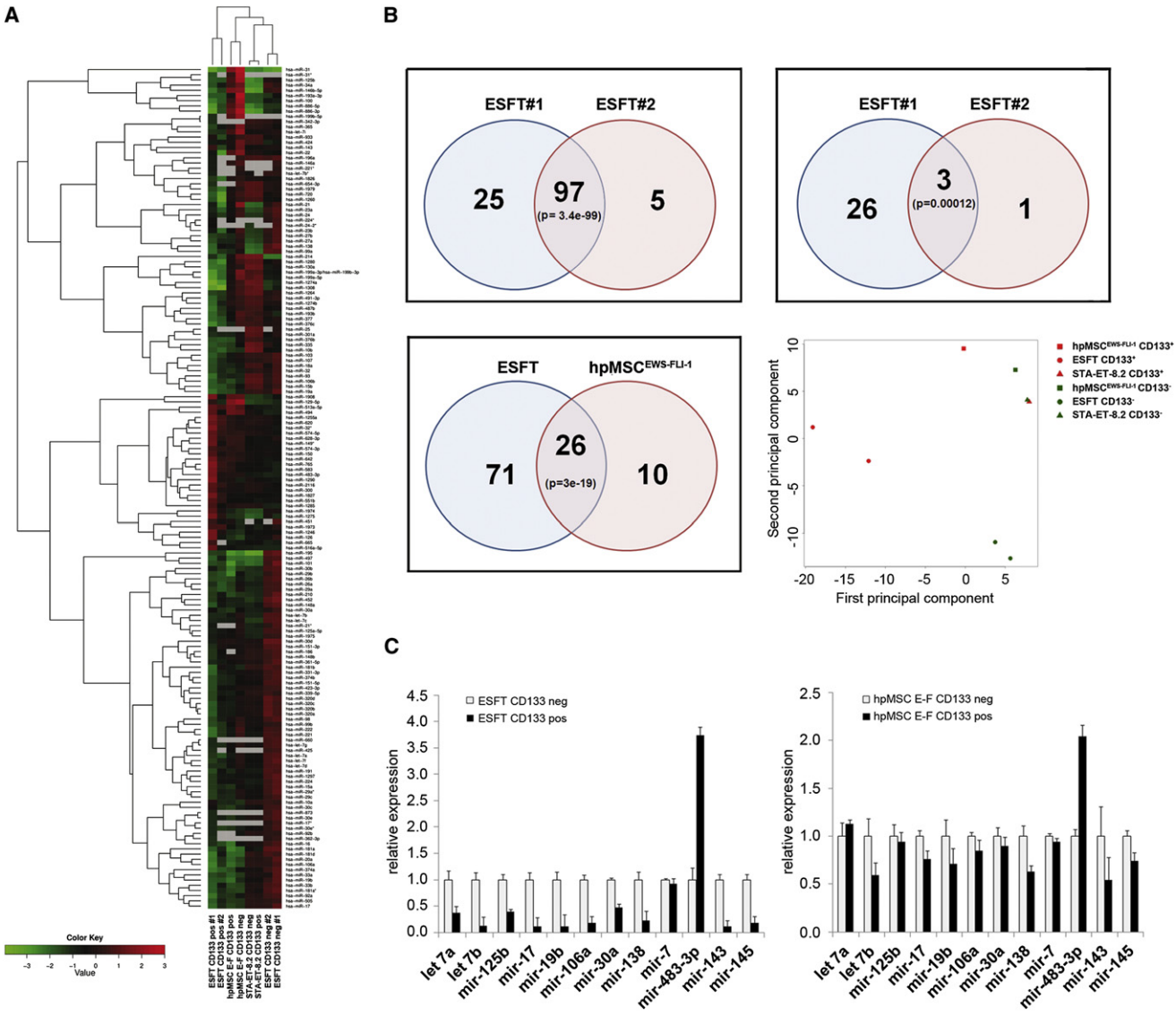

Figure 1. Mature miRNA Expression in ESFT

(A) Clustering of CD133$^+$ and CD133$^-$ hpMSC$^{EWS\text{-}FLI1}$, primary ESFT cells, and STA-ET-8.2 cells.

(B) Venn diagrams indicating shared repressed (top left) and induced (top right) miRNAs between primary CD133$^+$ cells from different ESFT samples, and shared repressed miRNAs between primary CD133$^+$ ESFT and hpMSC$^{EWS\text{-}FLI\text{-}1}$ cells (lower left). Principle of component analysis of the eight samples used is shown (lower right).

(C) Real-time PCR analysis of the expression of selected mature miRNAs in CD133$^+$ and CD133$^-$ primary ESFT cells (left) and hpMSC$^{EWS\text{-}FLI1}$ (right). Real-time PCR experiments were normalized to SNORD49a and were done in triplicate. Error bars represent the SD of three independent determinations.

See also Figure S1 and Tables S1, S2, S3, S4, and S5.

was observed with either primary ESFT CSC or hpMSC$^{EWS\text{-}FLI\text{-}1}$ CD133$^+$ cells (Figure 1A and Figure S1A). Established cell lines may therefore not be representative of CSCs, having adapted to in vitro culture conditions. Comparison of CD133$^+$ CSC and hpMSC$^{EWS\text{-}FLI\text{-}1}$ miRNA signatures to recently published miRNA expression profiles of normal human embryonic stem cells (hESCs), induced pluripotent stem cells (iPSCs), and fibroblasts (Wilson et al., 2009) showed that both CD133$^+$ populations share a significant portion of their miRNA repertoire with hESCs and iPSCs but not with fibroblasts (Table S2). Moreover, comparative analysis of ESFT CSCs and currently publicly available solid tumor miRNA CSC profiles, including those of hepatocellular (Ma et al., 2010b) (Table S3), prostate (Liu et al., 2011) (Table S4), and breast (Iliopoulos et al., 2011) (Table S5) carcinomas, revealed significant similarity. Thus, there appears to be marked molecular resemblance between ESFT CSCs, hESC/iPSCs, and CSCs from diverse tumor types, suggesting that the intrinsic stemness shared by these cells may rely on a common miRNA expression profile that overrides the differences in their ontogeny.

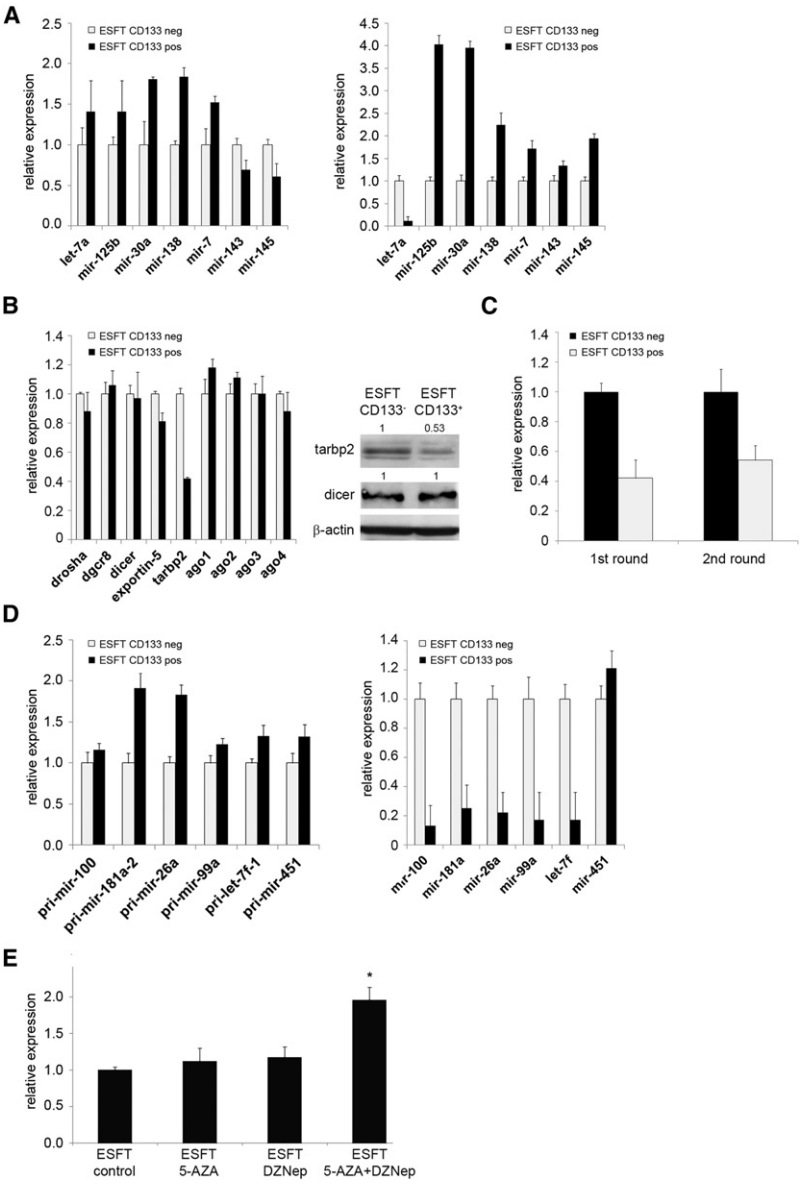

Figure 2. Tarbp2 Is Repressed in ESFT CSC

(A) Real-time PCR analysis of primary (pri-) miRNA expression (left) and primary and precursor (pre-) miRNA expression (right) in primary CD133$^+$ and CD133$^-$ ESFT cells.

(B) Left: Real-time PCR analysis of the expression of key components of the miRNA maturation machinery in primary CD133$^+$ and CD133$^-$ ESFT cells. Right: Western blot analysis of Tarbp2 and Dicer expression in primary ESFT CD133$^-$ and CD133$^+$ cells.

(C) Real-time PCR analysis of *TARBP2* expression in CD133$^+$ and CD133$^-$ ESFT cells after the first round of sorting from tumor samples and after ESFT sphere formation (second round of sorting).

(D) Real-time PCR analysis in primary CD133$^+$ and CD133$^-$ ESFT cells of the expression of primary (left) and mature (right) miRNAs that are regulated by Tarbp2 in both ESFT CSCs and colon cancer cells. Expression of the Tarbp2-independent miRNA-451 is included as an internal control.

(E) Real-time PCR analysis of *TARBP2* expression after 5 days of treatment with 5-AzaC (20 μM) and/or DZNep (10 μM). Real-time PCR experiments were normalized to 18S for mRNA or SNORD49a for miRNAs and were done in triplicate. Error bars represent the SD of three independent determinations. *p<0.05.

See also Figure S2.

ESFT CSCs Display Decreased TARBP2 Expression

Studies on Dicer KO mice showed that global reduction in miRNA processing and expression augments the tumorigenic potential of transformed cells (Kumar et al., 2007). Subsequent work suggested that defective miRNA biogenesis, resulting in a reduction in the amounts of their mature 21–23 nt form, is responsible for the repressed miRNA signature observed in cancer cells (Kumar et al., 2009). We hypothesized that the miRNA expression profile of CSC may reflect intrinsic deregulation of miRNA maturation, which could explain, at least in part, their phenotype and tumorigenic potential.

Expression of a panel of relevant pri-miRNAs, whose corresponding mature form was found to be repressed (Figure 1C), was assessed by qRT-PCR in CD133$^+$ and CD133$^-$ hpMSC$^{EWS\text{-}FLI\text{-}1}$, as well as in freshly isolated primary cells from ESFT 3 and 4. With the exception of the miRNA 143-145 cluster, which is known to be transcriptionally repressed by Oct-4, (Xu et al., 2009) no decrease in the tested pri-miRNA transcripts was observed in either of the CD133$^+$ populations (Figure 2A, left, and Figure S2A, left), indicating that, for most of the repressed mature miRNAs, the initial transcription step is not affected. Expression of combined pri- and pre-forms of each of a selected panel of miRNAs was assessed according to recently described methods (Shan et al., 2008) to exclude a possible blockade in the pri- to pre-miRNA maturation step. With the exception of let-7a, combined pri- and pre-miRNA levels were found to be increased in CD133$^+$ compared to CD133$^-$ cells (Figure 2A, right, and Figure S2A, right) for all species tested, consistent with pre-miRNA accumulation and a late miRNA maturation defect in CSCs. The strong decrease in combined let-7a pri- and pre-miRNA may be attributed to elevated expression of Lin28B in ESFT CSCs (De Vito et al., 2011), reported to act primarily on pre-let-7a (Piskounova et al., 2011).

Because CD133$^-$ cells are derived from their CD133$^+$ counterparts (Suvà et al., 2009), we reasoned that any miRNA maturation defect responsible for CSC development should be reversible. A putative underlying mechanism may therefore include altered transcriptional regulation of molecules implicated in miRNA biogenesis. Accordingly, we assessed the expression of *DROSHA, DGCR8, DICER, TARBP2, AGO1-4*, and *EXPORTIN5* by qRT-PCR in primary ESFT cells and hpMSC$^{EWS\text{-}FLI\text{-}1}$. Interestingly, the *TARBP2* transcript (Figure 2B, left), as well as the corresponding protein (Figure 2B, right), were significantly repressed in CD133$^+$ ESFT cells. The *TARBP2* transcript was also repressed in hpMSC$^{EWS\text{-}FLI\text{-}1}$ (Figure S2B), albeit less markedly

Table 1. Downregulated miRNAs Common to CD133$^+$ ESFT Cells and CD133$^+$ hpMSC$^{EWS\text{-}FLI\text{-}1}$ that Are Modulated in Colon Cancer-Bearing Mutated *TARBP2*

ESFT CD133 pos #1	ESFT CD133 pos #2	hpMSC$^{EWS\text{-}FLI\text{-}1}$ CD133 pos
hsa-miR-181a	hsa-miR-26a	hsa-miR-26a
hsa-miR-99a	hsa-miR-99a	hsa-miR-125b
hsa-let-7f	hsa-miR-181a	hsa-miR-100
hsa-miR-26a	hsa-miR-125b	Hsa-let-7f
hsa-miR-125b	hsa-let-7f	
hsa-miR-196a	hsa-miR-10a	
hsa-miR-100	hsa-miR-100	
p = 0.0063	p = 0.0022	p = 0.024

so than in primary CD133$^+$ ESFT cells, whereas no difference in *TARBP2* expression was observed between STA-ET-8.2-derived CD133$^+$ and CD133$^-$ fractions (data not shown). Among the other genes implicated in miRNA biogenesis tested, only *XPO5* was observed to be modestly repressed in CD133$^+$ ESFT cells, prompting us to focus on *TARBP2*.

ESFT CSCs Display a TARBP2 Expression-Dependent Defect in miRNA Maturation

The *TARBP2* gene encodes an integral component of a Dicer1-containing complex whose mutation has recently been reported to participate in the pathogenesis of sporadic and hereditary colon carcinomas with microsatellite instability (Melo et al., 2009). The observed frameshift mutations cause a decrease in Tarbp2 protein expression, which leads to a broad defect in miRNA maturation, possibly as a result of Dicer1 protein destabilization (Melo et al., 2009). To exclude the possibility that *TARBP2* downregulation in our CSC model might be due to mutation, primary ESFT *TARBP2* cDNA was sequenced and found to be wild-type (data not shown). Interestingly, Dicer1 expression was unaltered at the protein level in primary ESFT CD133$^+$ fractions (Figure 2B left), suggesting that the reduced Tarbp2 levels may suffice to maintain Dicer protein stability but not to ensure full Dicer complex function.

As previously observed (Suvà et al., 2009), only CD133$^+$ ESFT cells were able to generate spheres, which contain both CD133$^+$ and CD133$^-$ cell fractions. Similar to freshly isolated CD133$^+$ cells, sphere-derived CD133$^+$ cells displayed decreased *TARBP2* expression compared to their CD133$^-$ derivatives, highlighting the reversibility of *TARBP2* repression in CSC (Figure 2C).

The ESFT CSC miRNA signature revealed significant overlap with that observed upon *TARBP2* mutation in colon cancer cell lines (Melo et al., 2009) (Table 1), suggesting that the partial *TARBP2* repression identified in ESFT CSCs may underlie their defective miRNA maturation. qRT-PCR assessment of a panel of pri- and mature miRNAs, including miRNAs 100, 181a, 26a, 99a, and let-7f, reported to be part of the *TARBP2* miRNA profile in colon cancer cells, validated the molecular similarity suggested by array analysis, further supporting a putative implication of Tarbp2 in the generation of the ESFT CSC miRNA profile (Figure 2D). To verify that repression of miRNAs in ESFT CSCs results, at least in part, from a Tarbp2/Dicer-dependent maturation blockade, we measured by qRT-PCR the expression of miRNA-451, which has been shown to be processed in a Dicer-independent manner (Yang et al., 2010). No difference in miRNA-451 expression was observed between ESFT CD133$^+$ and CD133$^-$ cells (Figure 2D).

Given the reversibility of *TARBP2* repression in CD133$^+$ ESFT cells and preclusion of detailed promoter methylation analysis by the paucity of CD133$^+$ cells, we addressed possible epigenetic mechanisms that may underlie the observed *TARBP2* repression using a pharmacological approach. CD133$^+$ ESFT cells were subjected to treatment with 20 μM 5-Aza-2-deoxycytidine (5-AzaC), to block CpG island methylation in the *TARBP2* promoter, and with 10 μM of the S-adenosyl homocysteine hydrolase inhibitor 3-Deazaneplanocin A (DZNep), to block histone H3K27 and H3K9 methylation (Tan et al., 2007). The two reagents were applied alone or in combination for 5 days, and corresponding changes in *TARBP2* expression were assessed by qRT-PCR. Although neither reagent alone altered expression significantly, the combination of both resulted in a 2-fold increase in expression, de facto restoring expression to the level observed in CD133$^-$ cells (Figure 2E).

Interestingly, several miRNAs that are downregulated in ESFT CSCs are also repressed in relapsing tumors (Nakatani et al., 2012), including miRNA-34a, 224, 376a, and 26a (Figure S2).

TARBP2-Depleted ESFT Cell Lines Mimic ESFT CSC Behavior

To address its role in generating the miRNA expression profile observed in ESFT CSCs, as well as its involvement in their tumorigenic potential, *TARBP2* was depleted in three different ESFT cell lines using an shRNA approach. A 52%–60% reduction in *TARBP2* mRNA and protein expression, as assessed by qRT-PCR (Figure 3A, left) and western blot (Figure 3A, right) analysis, respectively, was obtained that corresponds to the difference in Tarbp2 expression levels observed between freshly isolated CD133$^+$ and CD133$^-$ ESFT cells. Similar to primary ESFT, Dicer protein expression was unaltered upon Tarbp2 depletion (Figure 3A). miRNA expression analysis of control vector-infected and sh*TARBP2*-expressing cells revealed that *TARBP2*-depleted cells acquire a miRNA profile that is remarkably similar to that of CD133$^+$ hpMSC$^{EWS\text{-}FLI\text{-}1}$ and ESFT CSCs (Figure 3B). Consistent with this observation, qRT-PCR analysis confirmed that expression of a panel of mature miRNAs regulated by Tarbp2 in both ESFT CSCs and colon cancer cells was repressed in *TARBP2*-depleted ESFT cell lines, without decreasing transcription of their corresponding pri-miRNA forms (Figure 3C, Figure S3A, and data not shown). miRNAs that were upregulated in CD133$^+$ cells were also upregulated in sh*TARBP2*-expressing cells, suggesting that the same or related internal regulatory pathways are modified in ESFT CSCs and ESFT cell lines upon *TARBP2* depletion.

Because *TARBP2*-depleted ESFT cell lines display a miRNA expression profile reminiscent of that of ESFT CSCs, we assessed the effect of *TARBP2* depletion on ESFT cell line proliferation and tumorigenicity. Although there was no significant difference in ESFT cell proliferation in vitro (Figure S3B), subcutaneous injection of control vector- and sh*TARBP2*-infected A673, TC252, and STA-ET-8.2 cells into six NOD-SCID mice each revealed accelerated tumor emergence from *TARBP2*-depleted cells (Figure 3D). The decreased *TARBP2* expression

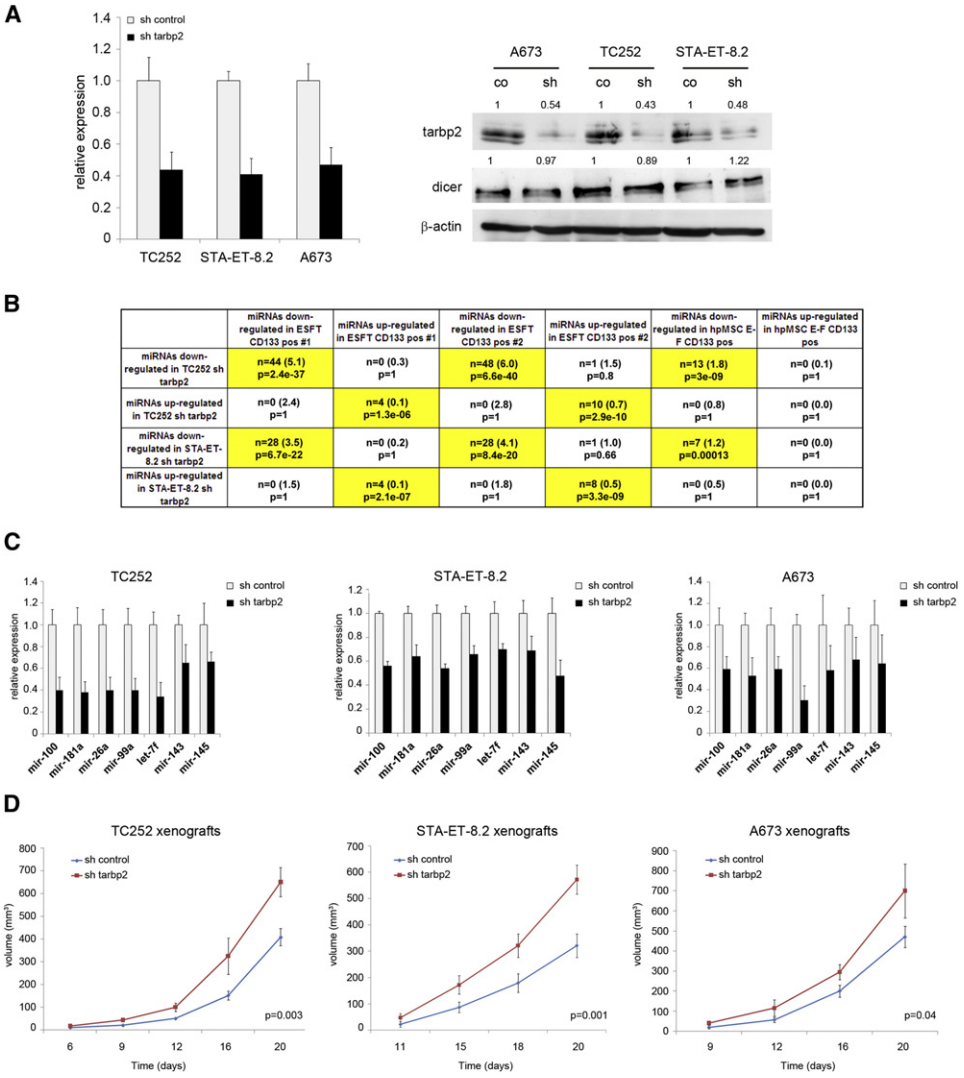

	miRNAs down-regulated in ESFT CD133 pos #1	miRNAs up-regulated in ESFT CD133 pos #1	miRNAs down-regulated in ESFT CD133 pos #2	miRNAs up-regulated in ESFT CD133 pos #2	miRNAs down-regulated in hpMSC E-F CD133 pos	miRNAs up-regulated in hpMSC E-F CD133 pos
miRNAs down-regulated in TC252 sh tarbp2	n=44 (5.1) p=2.4e-37	n=0 (0.3) p=1	n=48 (6.0) p=6.6e-40	n=1 (1.5) p=0.8	n=13 (1.8) p=3e-09	n=0 (0.1) p=1
miRNAs up-regulated in TC252 sh tarbp2	n=0 (2.4) p=1	n=4 (0.1) p=1.3e-06	n=0 (2.8) p=1	n=10 (0.7) p=2.9e-10	n=0 (0.8) p=1	n=0 (0.0) p=1
miRNAs down-regulated in STA-ET-8.2 sh tarbp2	n=28 (3.5) p=6.7e-22	n=0 (0.2) p=1	n=28 (4.1) p=8.4e-20	n=1 (1.0) p=0.66	n=7 (1.2) p=0.00013	n=0 (0.0) p=1
miRNAs up-regulated in STA-ET-8.2 sh tarbp2	n=0 (1.5) p=1	n=4 (0.1) p=2.1e-07	n=0 (1.8) p=1	n=8 (0.5) p=3.3e-09	n=0 (0.5) p=1	n=0 (0.0) p=1

Figure 3. Depletion of Tarbp2 in ESFT Cells Leads to an ESFT CSC miRNA Profile and Increases Tumorigenicity

(A) Real-time PCR (left) and western blot (right) analysis of *TARBP2* depletion in A673, TC252, and STA-ET-8.2 ESFT cell lines.

(B) Comparison of miRNA profiles between ESFT cell lines depleted of TARBP2, CD133^{+} ESFT cells, and CD133^{+} hpMSC$^{EWS\text{-}FLI1}$. N indicates the number of shared miRNAs by each cell population pair. The number of expected shared miRNAs is shown in brackets, and the p value is indicated. Statistically significant similarities are highlighted in yellow.

(C) Real-time PCR comparison of mature miRNA expression in *TARBP2*-depleted and control shRNA-treated ESFT cell lines.

(D) Growth curve of TC252 STA-ET-8.2 and A673 tumors depleted or not of *TARBP2*. Real-time PCR experiments were normalized to 18S for mRNA or SNORD49a for miRNAs and were done in triplicate. Error bars represent the SD of three independent determinations. Student's t test was used for statistical analysis.

See also Figure S3.

observed in ESFT CSCs may therefore be implicated in their tumorigenic potential.

To compare the effect of depleting *DICER* to that of depleting *TARBP2* on ESFT tumorigenicity, *DICER*-specific shRNA was stably expressed in the ESFT cell lines A673 and TC71 and resulted in a 42%–43% depletion of Dicer protein (Figure S3C). Neither cell viability nor proliferation (Figure S3D) was affected. However, xenografts of the cells in immunocompromised mice displayed a significant increase in tumorigenicity (Figure S3E) and downregulation of a panel of Tarbp2/Dicer-dependent miRNAs (Figure S3F).

Enoxacin Inhibits Tumor Development from ESFT Cell Lines

To address the potential effectiveness of restoring miRNA expression in inhibiting tumor growth, we explored methods of augmenting Tarbp2 function that may be applicable to therapy. The possibility to specifically enhance Tarbp2 activity, without affecting its expression level, has been recently demonstrated using enoxacin, an antibacterial agent of the fluoroquinolone family (Melo et al., 2011; Shan et al., 2008). We therefore assessed the effect of enoxacin on ESFT cell line miRNA expression in vitro and tumorigenesis in vivo. ESFT cell lines TC252,

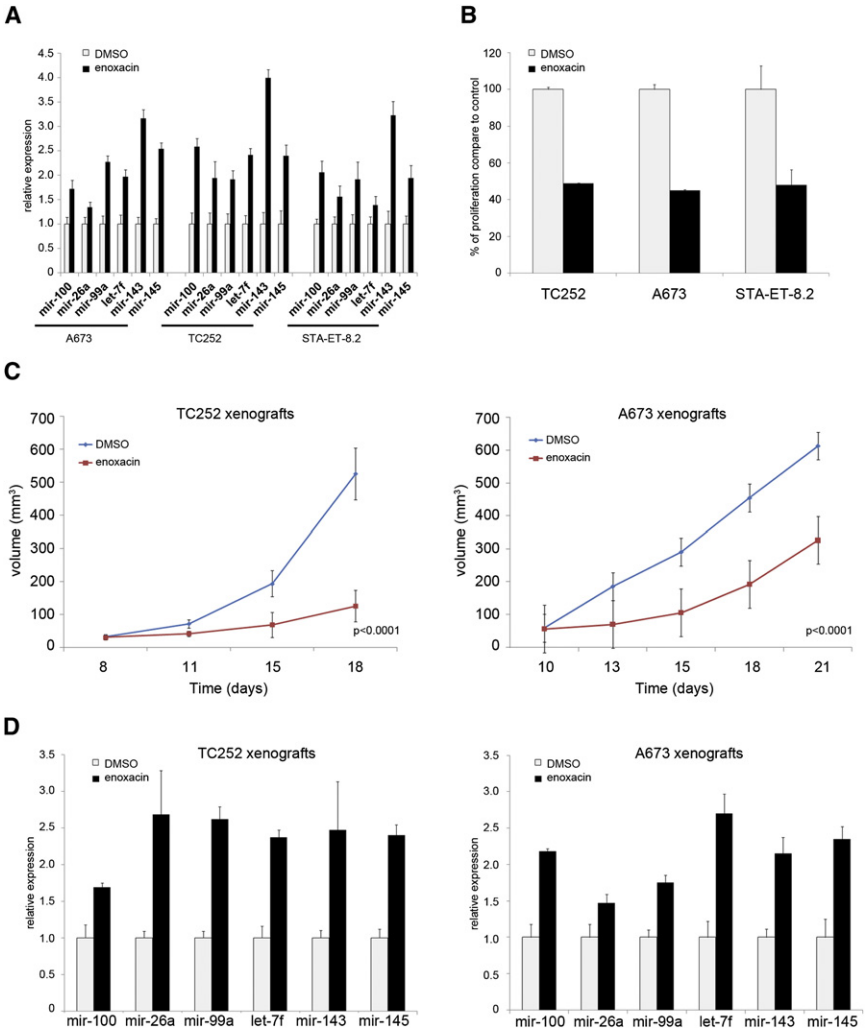

Figure 4. Enoxacin Blocks ESFT Cell Line Growth In Vivo

(A) Real-time PCR analysis of expression of a panel of mature Tarbp2-dependent miRNAs upon DMSO or 40 μg/ml enoxacin treatment of A673, TC252, and STA-ET-8.2 cells.

(B) MTT assay in DMSO- or enoxacin-treated (40 μg/ml) ESFT cells for 72 hr.

(C) Growth curves of established TC252 and A673 tumors in mice receiving daily i.p. enoxacin (10 mg/kg) or DMSO injections.

(D) Real-time PCR analysis of mature miRNA expression in DMSO- or enoxacin-treated tumors at autopsy. Real-time PCR experiments were normalized to SNORD49a and were done in triplicate. Error bars represent the SD of three independent determinations. Student's t test was used for statistical analysis.

See also Figure S4.

STA-ET-8.2, and A673 treated for 72 hr with enoxacin (40 μg/ml) showed an increase in Tarbp2-dependent miRNA expression (Figure 4A), without alteration of Tarbp2 expression itself (Figure S4). They also displayed significant reduction in their in vitro proliferation, as assessed by MTT assays (Figure 4B).

TC252 and A673 cells were injected subcutaneously into 12 NOD-SCID mice, and daily intraperitoneal treatment with enoxacin (n = 6) or solvent (DMSO, n = 6) was initiated at a dose of 10 mg/kg for a total of 10 days, once tumor volume reached 60 mm^3. Tumor growth was significantly inhibited in enoxacin-treated compared to DMSO-treated animals (Figure 4C). As expected, upregulation of Tarbp2-dependent miRNAs in enoxacin-treated tumors was observed (Figure 4D), consistent with the notion that enoxacin enhances endogenous Tarbp2 activity, which leads to increased miRNA maturation and inhibition of ESFT tumor growth.

Reconstitution of TARBP2 Expression and Function in ESFT CSC Impairs Their Self-Renewal In Vitro and Tumorigenic Potential In Vivo

We next addressed the effect of enoxacin on primary ESFT spheres. ESFT CSCs cultured as spheres in serum free conditions were treated with enoxacin (40 μg/ml) or solvent (DMSO) for 3 days, following which their clonogenic capacity, miRNA expression profile, and stem cell protein expression levels were assessed. Clonogenic assays revealed a 50% reduction in sphere formation by enoxacin-treated CSCs (Figure 5A). Enoxacin-treated spheres also displayed increased expression of a panel of Tarbp2/Dicer-dependent miRNAs (Figure 5B) and decreased expression of Oct-4, Nanog, and Sox-2 proteins (Figure 5C). To validate the notion that the effect of enoxacin was due to enhancement of Tarbp2 activity, we assessed the effect of *TARBP2* overexpression on ESFT spheres. Lentivirus-mediated introduction of *TARBP2* into primary ESFT spheres resulted in a marked decrease in their clonogenicity (Figure 5D) and a concomitant increase in the expression of a panel of Tarbp2-dependent miRNAs, including miRNAs 100, 181a, 26a, 99a, Let-7f, 143, and 145 (Figure 5E). Partial repression of Oct-4, Nanog, and Sox-2 (Figure 5F), comparable to that observed upon enoxacin treatment, was also noted. These observations indicate that enoxacin mimics the effect of exogenous *TARBP2* introduction and that enhanced Tarbp2 activity impairs ESFT CSC self-renewal.

To address the effect of restoring Tarbp2 activity on primary tumor growth and CSC population maintenance, 200,000 ESFT cells freshly isolated from ESFT 3, of which 15% were $CD133^+$, were injected beneath the renal capsule of 12 immunocompromised mice each. After 3 weeks of growth, six of the mice were treated with vehicle (DMSO) only, whereas the remaining six received daily injections of enoxacin at 10 mg/kg for 10 days. The mice were then sacrificed and tumors examined for size, morphology, and $CD133^+$ cell content. Although tumor size was comparable in control and enoxacin-treated animals (Figure 5G, left), control tumors were firm with little or no necrosis, whereas tumors from enoxacin-treated animals were

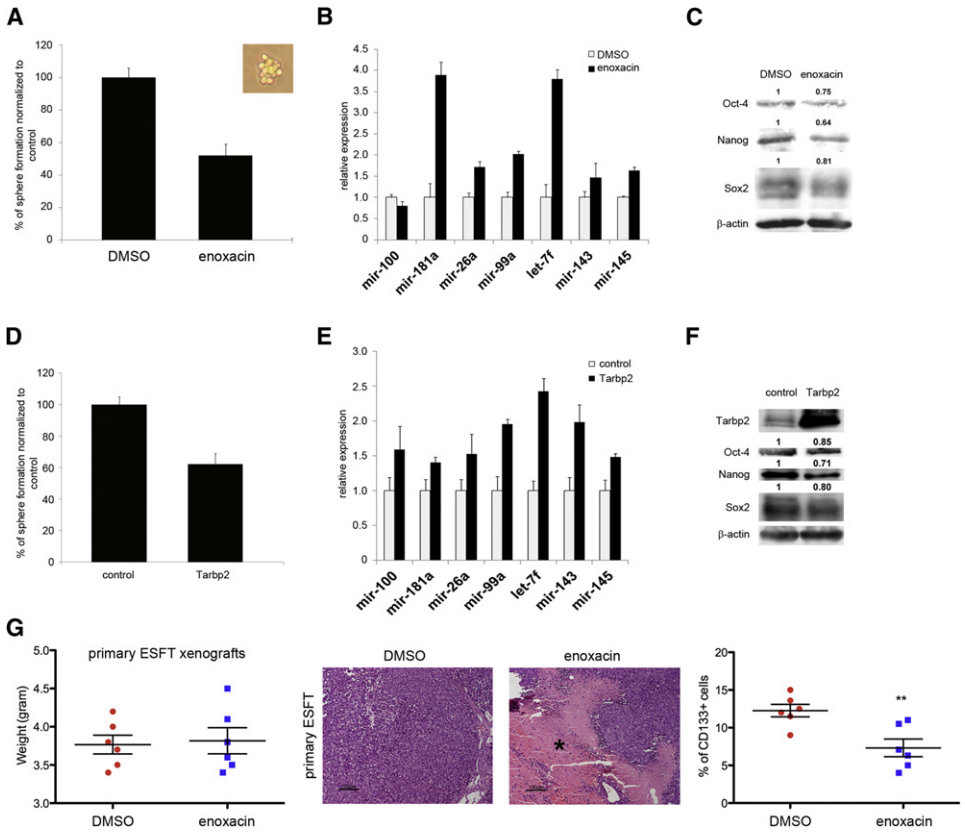

Figure 5. Enoxacin Treatment Inhibits ESFT CSC Self-Renewal In Vitro and Depletes CSC Populations In Vivo

(A) Clonogenic assay of DMSO- or enoxacin-treated primary ESFTs as assessed by sphere formation from single cell cultures. Sphere formation (inset) was scored after 30 days; 40 μg/ml of enoxacin was added to the cultures every 5 days.

(B) Real-time PCR analysis of expression of a panel of mature miRNAs in primary ESFT spheres treated with DMSO or enoxacin (40 μg/ml) for 5 days.

(C) Western blot analysis of Oct-4, Nanog, and Sox-2 proteins in primary ESFT spheres treated with DMSO or enoxacin (40 μg/ml) for 5 days.

(D) Clonogenic assay of primary ESFT cells overexpressing exogenous TARBP2, as assessed by sphere formation from single cell cultures. Sphere formation was scored after 30 days.

(E) Real-time PCR analysis of expression of a panel of mature miRNAs in primary control ESFT cells and ESFT cells overexpressing exogenous TARBP2.

(F) Western blot analysis of the expression of Tarbp2 and Oct-4, Nanog, and Sox-2 proteins in primary ESFT spheres infected with *TARBP2* cDNA-containing lentivirus.

(G) Left panel: weight of primary ESFT xenografts grown under the renal capsule for 3 weeks prior to daily i.p. injections of enoxacin (10 mg/kg) for 10 days. Middle panel: histology of DMSO- and enoxacin-treated tumors. The asterisk indicates necrosis. Scale bar = 100 μm. Right panel: fraction of viable cells from DMSO- and enoxacin-treated tumors expressing CD133. Real-time PCR experiments were normalized to SNORD49a and were done in triplicate. Error bars represent the SD of three independent determinations. $^{**}p < 0.005$.

soft and hemorrhagic with extensive necrosis (Figure 5G, middle). Importantly, the $CD133^+$ cell subpopulation was reduced from 15% to 7% (Figure 5G, right).

miRNA-143 and miRNA-145 Control ESFT CSC Self-Renewal and Tumorigenicity

ESFT spheres cultured in the presence of serum for 1 week become adherent, acquire an elongated MSC-like phenotype, and lose their tumorigenic potential (Figure 6A). We therefore compared the miRNA expression profile of spheres and their adherent cell counterparts from two different ESFTs (Figure 6B). Similar to ESFT $CD133^+$ and $CD133^-$ cells, PCA analysis showed that spheres and adherent cells from the two populations cluster together, respectively (Figure S5). Compared to their adherent counterparts, ESFT spheres displayed upregulation of the known oncogenic 17-92a miRNA cluster (Figure 6B and C), whereas the *TARBP2*-dependent miR-143/miR-145 cluster (Melo et al., 2011) was among their most strongly repressed miRNAs (Figure 6B and C). miRNA expression profile differences between spheres and adherent cells were not identical to those observed between primary $CD133^+$ and $CD133^-$ ESFT cells, because spheres are composed of both $CD133^+$ and $CD133^-$ cells. Moreover, comparison of spheres and adherent cells highlights serum-induced differences in differentiation and tumorigenicity, whereas comparison between $CD133^+$ and $CD133^-$ cells underscores differences in stemness. miRNAs that show similar expression differences in the two comparisons are therefore likely to be relevant to CSC constitution and maintenance.

Having previously shown that miRNA-145 plays an important role in the generation of ESFT CSCs and in ESFT tumorigenicity (Riggi et al., 2010), we addressed the function of the miRNA

143-145 cluster in ESFT CSC self-renewal. By introducing the cluster into primary ESFT spheres using a lentiviral system, we obtained a 260- and 220-fold expression of miRNA-143 and miRNA-145, respectively (Figure 6D). Clonogenic assays showed that both miRNA-143- and miRNA-145-overexpressing-ESFT spheres have lower self-renewal capacity (Figure 6E) that correlates with suppression of *OCT4* and *NANOG* but not *SOX2* transcripts (Figure 6F). Although *SOX2* is a target of miRNA-145, its response to changes in miRNA-145 expression may occur at the transcriptional or translational level and may vary according to cell type (Xu et al., 2009). Downregulation of the miRNA 143-145 cluster therefore appears to play an important role in ESFT CSC self-renewal.

Because both miRNA-143 and miRNA-145 impair in vitro ESFT CSC self-renewal, we assessed whether, similar to miRNA-145, miRNA-143 could inhibit ESFT tumorigenicity. The introduction of miRNA-143 into ESFT cell lines A673 and TC252 resulted in a 150- to 200-fold increase in its expression, respectively (Figure 7A). Although proliferation was only minimally affected (Figure 7B), subcutaneous injection of control vector-infected or miRNA-143-overexpressing ESFT cells into six NOD-SCID mice each revealed that miRNA-143 overexpression significantly reduced ESFT tumor growth in vivo (Figure 7C). Because exogenous miRNA administration has been shown to effectively control tumor growth in experimental models (Ma et al., 2010a; Wiggins et al., 2010), we asked whether systemic injection of synthetic miRNAs can block or reverse growth of established tumors. Similar to in vivo treatment using enoxacin, miRNA-based treatment was initiated once the tumor reached a volume of 60 mm^3. Tail vein injection of 30 μg of synthetic miRNA-143 or miRNA-145 was administrated on days 11, 14, and 18. Mice treated with either miRNA-143 or miRNA-145 showed significant reduction of tumor volume compared to control-treated animals (Figure 7D). To verify that synthetic miRNAs had reached the tumors, total RNA was extracted from the tumors, and expression of miRNA-143 and miRNA-145 were assessed by qRT-PCR (Figure 7E), along with the expression level of the known miRNA-145 target genes *OCT4* and *KLF4* (Figure 7F). A 2-fold increase in miRNA-143 and miRNA-145 expression, along with a significant decrease in of *OCT4* and *KLF4* expression levels, were found in the treated tumors.

DISCUSSION

A Common miRNA Signature and Functionally Related miRNAs May Underlie and Sustain the CSC Phenotype

Although broad miRNA repression is a well-established feature of malignant cells, there has been little evidence of shared miRNA profiles among different cancer types. The present study demonstrates that the miRNA profile of $CD133^+$ ESFT CSC and $hpMSC^{EWS\text{-}FLI\text{-}1}$ populations is at least partially shared by hESCs and iPSCs, but not by terminally differentiated fibroblasts, consistent with the notion that their stem cell properties reflect a common intrinsic molecular profile. Greater similarity was observed between miRNA expression profiles of ESFT CSCs and hepatocellular, breast, and prostate carcinoma CSCs than between those of $CD133^+$ $hpMSC^{EWS\text{-}FLI1}$ and the different carcinomas. This may reflect the distinction between cells of origin of a tumor that incur the initial transforming events to become tumor initiating cells (TICs) and CSCs that represent the self-renewing and tumor-sustaining population in the established tumor (Visvader, 2011). The observed miRNA expression profile similarity between $CD133^+$ $hpMSC^{EWS\text{-}FLI\text{-}1}$ and ESFT CSCs suggests that $CD133^+$ $hpMSC^{EWS\text{-}FLI\text{-}1}$ may represent early stages of ESFT TIC generation that retain traces of the miRNA expression profile of the cell of origin. These traces may be diluted in established CSCs, whose miRNA profile more strongly reflects their transformed stem-cell-like properties.

Our observations indicate that miRNA expression signatures shared by CSCs from highly divergent tumor types not only resemble those of ESCs and iPSCs but may underlie and help sustain their phenotype and functional properties. Several studies have shown that an ESC-like transcriptional signature is associated with the most aggressive and undifferentiated form of cancers of diverse origin, suggesting the existence of a shared core pluripotency gene network. This putative network is composed of the target gene repertoire of a limited group of stem cell-related transcription factors, namely the Core, Polycomb, and c-Myc modules (Ben-Porath et al., 2008; Kim et al., 2010; Wong et al., 2008).

The core module is composed of target genes regulated by, among others, Oct-4, Nanog, Klf-4, Sox-2, and Lin-28; whereas the PRC module comprises Suz12, Ezh1/2, and Eed; and the c-Myc module includes Max and Rex1 (Wong et al., 2008). Each of these genes or group of genes is silenced by miRNAs found to be repressed in ESFT CSC. Thus, miRNA-145 represses *OCT4*, *KLF4*, and *SOX2* (Xu et al., 2009); let-7a silences *MYC* and *LIN28* (Kim et al., 2009) and is itself silenced by *LIN28* (Viswanathan et al., 2008); miRNA-26a controls *MYC* and *EZH2* (Sander et al., 2008); and miRNA-101 represses *EZH2* (Varambally et al., 2008). Furthermore, miRNA-145 is repressed in breast (Iorio et al., 2005) and colorectal cancer (Schepeler et al., 2008), miRNA-26a expression is reduced in hepatocellular carcinoma (Chen et al., 2011), let-7 repression is associated with lung cancer development (Trang et al., 2010), whereas miRNA-101 is downregulated in prostate (Varambally et al., 2008), liver (Su et al., 2009), and bladder cancer (Friedman et al., 2009). A plausible scenario may therefore be that deregulation of a restricted set of ESC-related miRNAs may govern expression of different transcription modules, which help generate and sustain the CSC population. The miRNA signatures, however, need not be identical. Because expression of numerous transcripts can be regulated by different miRNAs, it is conceivable that CSC derived from diverse tumor types, and therefore generated by distinct oncogenic events, may exploit different miRNAs to modulate expression of an identical set of transcription factors that are required for their survival. For example, ESFT- and breast cancer-derived CSC appear to share the same let-7a-mediated regulation of c-*myc* (Yu et al., 2007), whereas for the Polycomb group proteins, they use miRNA-26a/101 (Sander et al., 2008; Varambally et al., 2008) and miRNA-200 (Shimono et al., 2009), respectively.

Reversible Deregulation of TARBP2 Expression Determines CSC miRNA Profiles and Tumor Growth

Mutations in *TARBP2* have been identified in colon cancer associated with microsatellite instability (Melo et al., 2009). The resulting decrease in Trbp expression is associated with Dicer1

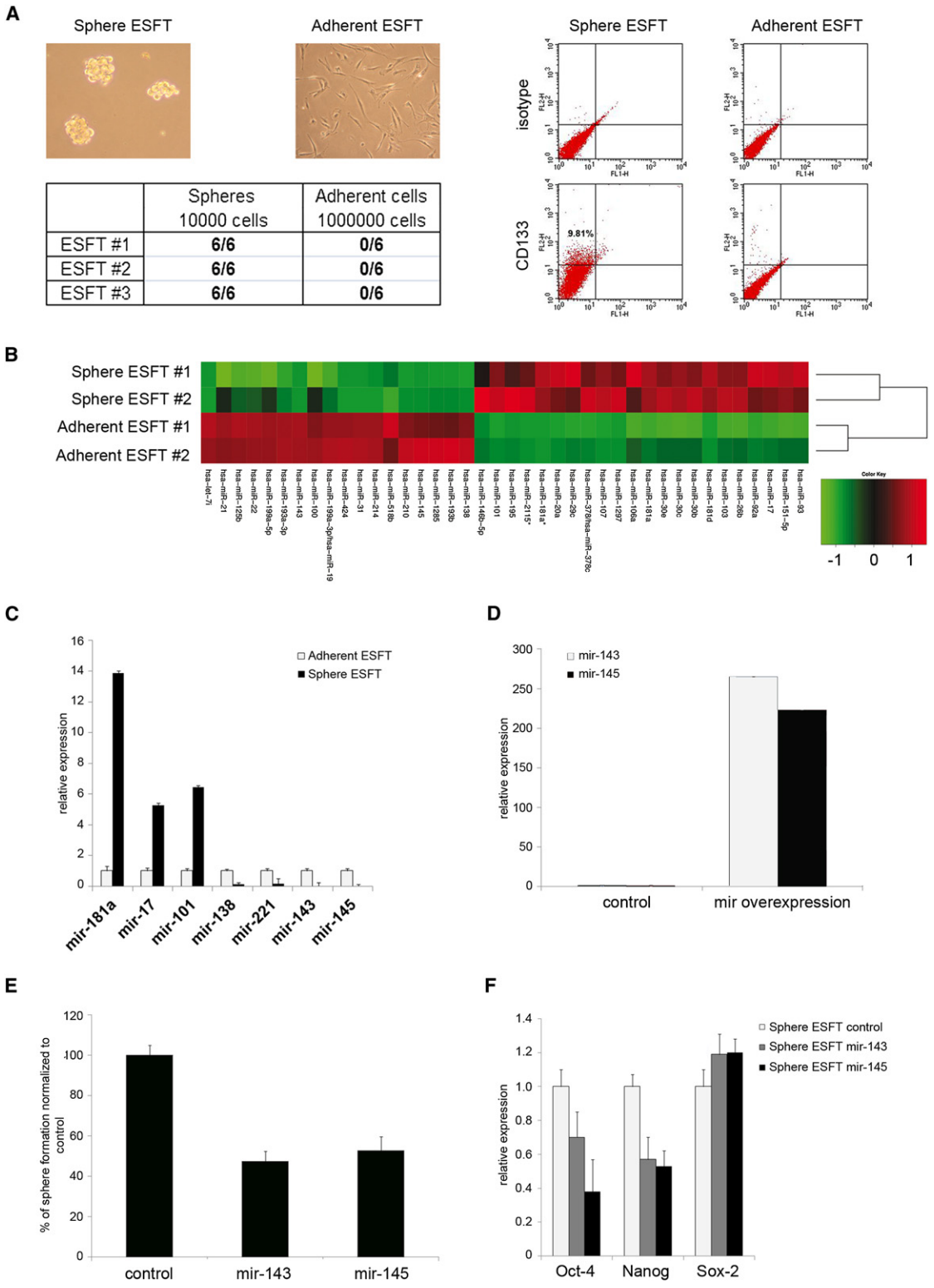

Figure 6. miRNA-143 and miRNA-145 Are Repressed in ESFT Spheres

(A) Upper left panel: ESFT sphere and adherent cell cultures are shown. Lower left panel: Tumor development following subcapsular kidney injection of primary ESFT spheres and adherent cells. The number of cells injected and the number of mice that developed tumors are indicated. Cells from three independent primary ESFTs were used. Right panel: Flow cytometry analysis of CD133 expression in ESFT spheres and adherent cell cultures.

(B) Clustering of primary ESFT spheres and adherent ESFT cells.

(C) Real-time PCR comparison of the expression of a panel of mature miRNAs in primary ESFT spheres and adherent ESFT cells.

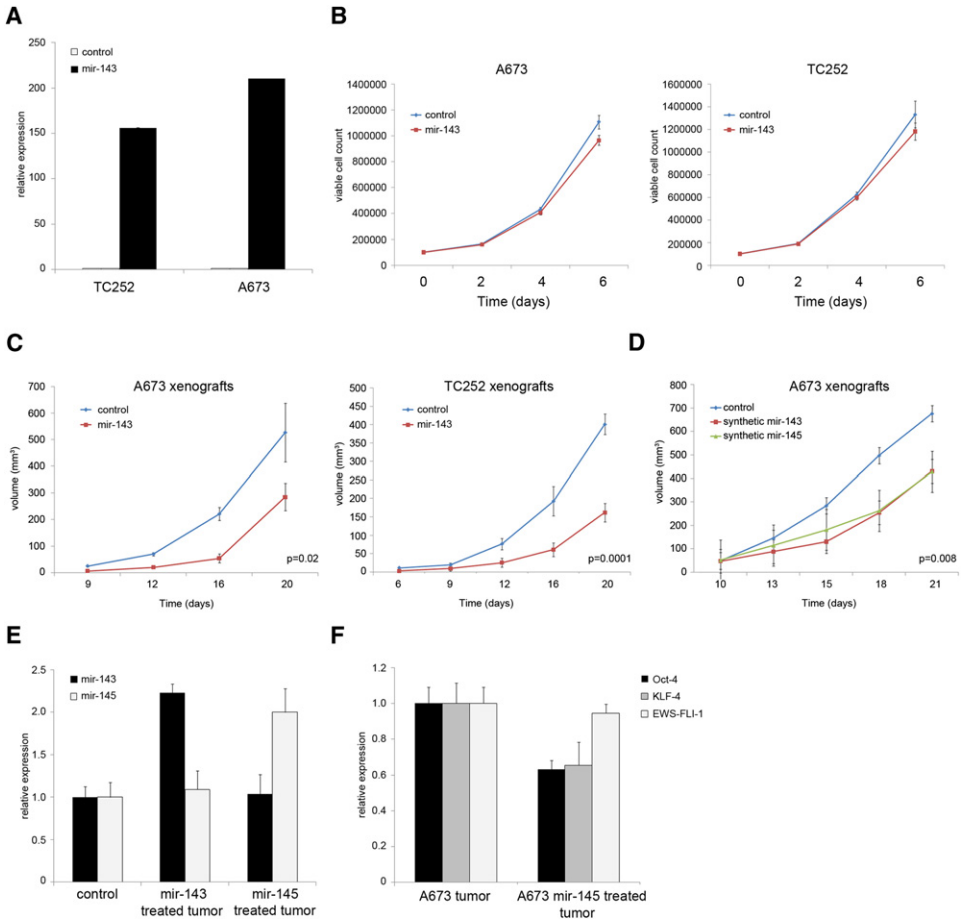

Figure 7. Synthetic miRNA-143 and miRNA-145 Inhibit ESFT Tumor Growth

(A) miRNA-143 overexpression in TC252 and A673 ESFT cells following retroviral introduction.

(B) Curve growth of control and miR-143 overexpressing A673 and TC252 cells.

(C) Tumor growth curves in six mice each from miRNA-143 and empty vector-infected A673 and TC252 cells.

(D) Growth curves of established A673 tumors in mice treated by tail vein injection of 30 μg of synthetic miRNA-143 or miRNA-145. miRNA-143 or miRNA145 was administered on days 11, 14, and 17 following subcutaneous A673 cell injection. Mice were sacrificed on day 20, and tumor size was assessed.

(E) Real-time PCR analysis of miRNA-143 and miRNA-145 expression in A673 tumors from miRNA-treated or control mice.

(F) Real-time PCR analysis of *OCT4* and *KLF4* expression in tumors from miRNA-145 treated or control mice. Real-time PCR experiments were normalized to SNORD49a for miRNA or 18S for mRNA and were done in triplicate. Error bars represent the SD of three independent determinations. Student's t test was used for statistical analysis.

protein instability or Dicer complex dysfunction that leads to defective miRNA processing (Chendrimada et al., 2005). Interestingly, the degree of reduction in Trbp expression observed in colon cancer cells corresponds to the 50% lower expression in CD133$^+$ ESFT CSCs compared to CD133$^-$ cells seen here. The notion that partial *TARBP2* repression may underlie the miRNA expression profile in ESFT CSCs is supported by the observation that shRNA-mediated depletion, by roughly 50%, of *TARBP2* in ESFT cell lines results in a miRNA expression profile that is highly reminiscent of that of ESFT CSCs, along with an increase in their tumorigenic potential. Furthermore, both introduction of exogenous *TARBP2* and enhancement of endogenous Tarbp2 activity by enoxacin resulted in reexpression of the broad panel of repressed miRNAs in ESFT CSCs, in addition to decreased clonogenicity. After 10 days of enoxacin treatment, CSC-derived tumors displayed massive necrosis, hemorrhage, and, most importantly, a roughly 50% decrease in the CD133$^+$ cell population. The extent of the necrosis observed is consistent with the notion that, in addition to promoting CSC differentiation, reconstitution of Tarbp2 activity

(D) Expression of miRNA-143 and miRNA-145 following lentiviral vector-mediated introduction into primary ESFT cells.

(E) Clonogenic assay showing reduced self-renewal of miRNA-143- and miRNA-145-overexpressing-ESFT cells.

(F) Real-time PCR analysis of *OCT4*, *NANOG*, and *SOX2* in empty vector-infected and miRNA-143 or miRNA-145 overexpressing primary ESFT spheres. Real-time PCR experiments were normalized to 18S for mRNA or SNORD49a for miRNAs and were done in triplicate. Error bars represent the SD of three independent determinations.

See also Figure S5.

drives a substantial proportion of the cells that constitute the tumor bulk toward death. One among several possible mechanisms may be downregulation of EWS-FLI-1 expression by miRNA-145 (Riggi et al., 2010), which could reduce the oncogenic driving force in both CSC and non-CSC populations, resulting in impairment of their growth and survival. Consistent with this view, the effect of enoxacin on cell line-derived tumors, which may at least partially mimic the tumor bulk, was to inhibit their growth.

Our observations suggest that partial inhibition of Tarbp2 function may constitute a key component of the mechanism that underlies defective miRNA maturation required for the emergence and maintenance of the CSC phenotype. Interestingly, the observed repression of *TARBP2* was not accompanied by Dicer protein instability, as assessed by western blot analysis, suggesting that partial *TARBP2* repression may deregulate the function of the Dicer complex without augmenting Dicer degradation itself. Alternatively, there may be a Tarbp2 repression range within which effects on miRNA expression are Tarbp2 specific. As expected, Dicer depletion by shRNA resulted in augmented tumorigenicity of ESFT cell lines, similar to the effect of Tarbp2 depletion, underscoring the importance of miRNA biogenesis in determining the tumorigenic potential of ESFT independently of the mechanisms that underlie initial transformation.

Robust upregulation of repressed Tarbp2-dependent miRNAs upon exposure of CSCs to serum indicates that the mechanisms underlying the defect in *TARBP2* expression are reversible. Consistent with this notion, we found that *TARBP2* expression could be restored by treating $CD133^+$ ESFT cells with a combination of 5-AzaC and DZNep, which suggests that *TARBP2* repression in these cells is likely due to a combination of DNA and histone methylation. Modulation of miRNA maturation as a means of altering expression of a broad panel of genes that orchestrate the full spectrum of CSC properties may provide tumor cells with a relatively simple way to acquire or lose the CSC phenotype. Epigenetic regulation of *TARBP2* expression may therefore constitute an important molecular switch that allows tumor cells to gain or relinquish CSC status in response to intrinsic or microenvironmental signals. Such regulation could maintain CSC as dynamic rather than fixed populations and account for their temporal and intertumor type size variability.

The similarities we have uncovered between miRNAs that are repressed in CSCs and in relapsing ESFT patients are consistent with the notion that CSCs constitute the population that is resistant to current chemotherapeutic agents and whose survival upon treatment is likely to be responsible for tumor relapse. The recent identification of miRNA-34a, the most robust event-free predictor miRNA in ESFT (Nakatani et al., 2012), as a p53 downstream target whose repression enhances somatic cell reprogramming and iPSC generation (Choi et al., 2011) further supports a potentially important mechanistic link between Tarbp2-dependent miRNA expression, CSC maintenance, and resistance to therapy in human tumors.

Targeting of Selected miRNAs Provides a Means to Control ESFT Growth

The miRNA 143-145 cluster has been observed to display tumor suppressor properties and to be downregulated in a broad range of tumor types (Tong and Nemunaitis, 2008). Moreover, we have previously shown the involvement of miRNA-145 in the generation of a $CD133^+$ subpopulation of $hpMSC^{EWS\text{-}FLI\text{-}1}$ that display CSC features (Riggi et al., 2010). Here, we demonstrate that both miRNA-145 and miRNA-143 are strongly repressed in ESFT CSCs and that their reexpression impairs self-renewal. miRNA-145 induction upon ESFT sphere exposure to serum may result in *OCT4* and *SOX2* repression, thereby inducing CSC differentiation and leading to loss of their tumor-initiating and -sustaining properties. In addition, miRNA-145 can repress EWS-FLI-1 expression (Riggi et al., 2010), neutralizing ESFT CSCs by at least two mechanisms: induction of differentiation on the one hand and silencing of the key oncogene on the other.

Taken together, our observations provide a plausible scenario for the emergence of CSCs in ESFTs. Expression of EWS-FLI-1 in appropriate primary host cells suppresses the miRNA 143-145 cluster, leading to genetic reprogramming that induces expression of *OCT4*, *NANOG*, and *SOX2*. The resulting network of induced target genes may modify the epigenetic landscape of EWS-FLI-1-expressing cells, leading to partial *TARBP2* suppression, which results in defective maturation of a host of miRNAs and the acquisition of the full-blown CSC phenotype. Depending on microenvironmental conditions, these cells may reexpress *TARBP2* and lose their tumorigenic potential, whereas others that are nontumorigenic may undergo partial *TARBP2* depletion and acquire or regain CSC features. Given the power of miRNA-driven gene expression to override the oncogenic effect of genetic mutations, restoration of relevant miRNA expression by systemic administration of synthetic miRNAs or correction of the underlying transient maturation defect may provide a potential means to control malignant growth. Effective therapy for any malignancy that harbors CSCs should simultaneously target the CSC population, to hamper tumor progression, as well as the bulk of the tumor to avoid the possibility that differentiated cells become reprogrammed toward the CSC phenotype. Increasing Tarbp2 activity by enoxacin may force ESFT CSCs to differentiate, while abrogating the opportunity for differentiated tumor cells to modulate their miRNA repertoire and to revert their phenotype to that of CSCs.

EXPERIMENTAL PROCEDURES

Cell Culture, Retroviral and Lentiviral Infection, and Tarbp2 Construct

Human pediatric mesenchymal stem cells (hpMSCs) were isolated and cultured as previously described (Riggi et al., 2010). A673 (ATCC), TC252 (kindly provided by Dr. T. Triche), STA-ET-8.2 (kindly provided by Dr. H. Kovar), and TC71 (kindly provided by Dr. E. De Alava) ESFT cells lines were cultured in RPMI (GIBCO) supplemented with 10% FCS (GIBCO). HpMSC, A673, TC252, STA-ET-8.2, and TC71 cells were infected as previously described (Riggi et al., 2010). MiR-143 vector was kindly provided by Dr. R. Agami. For stable knock-down of Tarbp2 (V3LHS_300582), pGIPZ lentiviral system from Open Biosystems was used. For stable knock-down of Dicer pSicoR sh dicer#1 (Addgene plasmid 14763) was used. Primary ESFT samples were obtained at surgery with approval of the ethics committee of the Canton de Vaud. All human samples were deidentified prior to analysis and were exempt from informed consent in accordance with the law of the Canton de Vaud. Spheres were cultured in IMDM (GIBCO), supplemented with 20% KO serum (GIBCO), 10 μg/ml LIF (Millipore), 10 ng/ml recombinant human epidermal growth factor (Invitrogen), and 10 ng/ml recombinant human basic fibroblast growth factor (Invitrogen). Single ESFT cell suspensions were infected using lentivirus-expressing miRNA control and mir-143-RFP (Biosettia) or miRNA-control

and mir-145-GFP (System Biosciences). *TARBP2* was amplified from cDNA of A673 cells and cloned into pLiV lentiviral vector.

RNA Isolation and Real-Time PCR

Total RNA was isolated using Trifast (Peqlab) according to the manufacturer's recommendations. Real-time PCR was performed as previously described (Riggi et al., 2010). TaqMan probes included 18S, *OCT4*, *NANOG*, *DROSHA*, *DICER*, pri-mir-138-1, and pri-mir-17 (Applied Biosystems). Primer sequences for SYBR Green gene expression quantification are listed in Supplemental Experimental Procedures. For microRNA quantification, 30 ng of total RNA was amplified using miRCURY LNA Universal RT microRNA PCR kit (Exiqon, DK) according to the manufacturer's recommendations. LNA PCR primers from Exiqon were used for RT-PCR amplification, and snord49a provided the endogenous control.

MicroRNA Array Profiling

Total RNA quality was verified by an Agilent 2100 Bioanalyzer profile. Total sample and reference RNA was labeled with Hy3 and Hy5 fluorescent label, respectively, using the miRCURY LNA Array power labeling kit (Exiqon, Denmark) according to the manufacturer's recommendations. Hy3-labeled samples and a Hy5-labeled reference RNA sample were mixed pairwise and hybridized to the miRCURY LNA array version sixth generation (Exiqon, Denmark), which contains capture probes targeting all miRNAs for human, mouse, or rat registered in the miRBASE version 16.0 at the Sanger Institute. Hybridization was performed according to the miRCURY LNA array manual using a Tecan HS4800 hybridization station (Tecan, Austria). The miRCURY LNA array microarray slides were scanned using the Agilent G2565BA Microarray Scanner System (Agilent Technologies, Inc., USA) and image analysis was performed using the ImaGene 9.0 software (BioDiscovery, Inc., USA). The quantified signals were background corrected and normalized using the global Lowess (LOcally WEighted Scatterplot Smoothing) regression algorithm.

Analysis of Microarray Data

Normalization of the microarray data was performed with the global Lowess regression algorithm. MicroRNAs showing expression fold-change greater than 2 (1.5 for the TARBP2-silenced cell lines) were considered differentially expressed. Clustering analysis was performed using average-linkage hierarchical clustering based on Pearson correlation coefficient. The statistical significance of the overlap between our microRNA lists and published ones was established in all cases using a one-sided exact Fisher test and Bonferroni correction for multiple testing.

Western Blots and Chemical Compounds

Western blots were performed according to standard procedures. Antibodies used for the study were anti-Tarbp2 (Abnova), anti-Dicer (Santa Cruz), anti-OCT-4 (Santa Cruz), anti-Nanog (R&D), anti-Sox2 (Chemicon Millipore), and anti-β-actin (Sigma). Quantification of bands was performed using imageJ Software. ESFT spheres were treated with 5-AzaC 20 μM (Sigma) and/or 3-Deazaneplanocin A (DZnep) 10 μM for 5 days.

Tumorigenicity Assays

Six NOD/SCID IL2 receptor common γ-chain knockout mice were anesthetized, and sphere-derived or adherent ESFT cells were injected beneath the renal capsule. All mice were sacrificed 3 months later, and the kidneys were removed at autopsy for histological analysis.

For assessment of the tumorigenic potential of TARBP2 depletion and miRNA-143-overexpression ESFT cells, NOD-SCID mice were anesthetized, and 1×10^6, 2×10^6, or 3×10^6 A673, TC252, or STA-ET-8.2 cells, respectively, were injected subcutaneously into six mice each. For assessment of the tumorigenic potential of Dicer depletion, NOD-SCID mice were anesthetized, and 1×10^6 or 4×10^6 A673 or TC71 cells, respectively, were injected subcutaneously into six mice each. The animals were sacrificed 4 weeks after injection. All tumors were removed at autopsy and sectioned for histological analysis. For in vivo treatment assays, 30 μg of miScript microRNA mimic (QIAGEN) were formulated with MaxSuppressor in vivo RNALancerII (BIOO Scientific, Inc), according to the manufacturer's recommendations. miRNAs were administrated intravenously by tail vein injection on days 11, 14, and 18. Tumor volume was measured as previously described (Esquela-Kerscher et al., 2008). Experimental protocols involving mice were approved by the Etat de Vaud, Service Vétérinaire, authorization number VD1942.1.

Cell Growth, Magnetic Cell Sorting, and FACS Analysis

ESFT cell lines were plated in triplicate wells and total cell counts and cell viability determined using trypan blue. The MTT assay was performed according to standard procedures. Magnetic cell sorting and FACS analysis were performed as previously described (Suvà et al., 2009).

Clonogenic Assays

Empty vector-infected, miRNA-143-RFP- or miRNA-145-GFP-expressing ESFT cells were plated as single cells in four 96-well plates and were cultured for 30 days in IMDM, 20% KO serum, LIF, EGF, and FGF. Sphere formation was scored 30 days later.

ACCESSION NUMBER

The Gene Expression Omnibus accession number for the miRNA expression profiles reported in this article is GSE31146.

SUPPLEMENTAL INFORMATION

Supplemental Information includes five figures, five tables, and Supplemental Experimental Procedures and can be found with this article online at doi:10.1016/j.ccr.2012.04.023.

ACKNOWLEDGMENTS

We thank Dr. T. Jacks for providing the pSicoR sh Dicer construct and Esther Rheinbay for graphic design. This work was supported by Swiss National Science Foundation (Grant 310030_130350), Oncosuisse (Grant 02158), the NCCR Molecular Oncology (to I.S.), and the Swiss Institute for Experimental Cancer Research Foundation (to I.S.). N.R. was supported by the Nuovo-Soldati Foundation and the Fonds Suisse Bourse Medecine et Biologie (Grant PASMP_134375/1). S.C. was supported by the FNS (MD-PhD Grant 323630-133894). P.P. was supported by the Italian Association for Cancer Research (Grant IG9408).

Received: June 30, 2011
Revised: January 12, 2012
Accepted: April 9, 2012
Published: June 11, 2012

REFERENCES

Bartel, D.P. (2009). MicroRNAs: target recognition and regulatory functions. Cell *136*, 215–233.

Ben-Porath, I., Thomson, M.W., Carey, V.J., Ge, R., Bell, G.W., Regev, A., and Weinberg, R.A. (2008). An embryonic stem cell-like gene expression signature in poorly differentiated aggressive human tumors. Nat. Genet. *40*, 499–507.

Chen, L., Zheng, J., Zhang, Y., Yang, L., Wang, J., Ni, J., Cui, D., Yu, C., and Cai, Z. (2011). Tumor-specific expression of microRNA-26a suppresses human hepatocellular carcinoma growth via cyclin-dependent and -independent pathways. Mol. Ther. *19*, 1521–1528.

Chendrimada, T.P., Gregory, R.I., Kumaraswamy, E., Norman, J., Cooch, N., Nishikura, K., and Shiekhattar, R. (2005). TRBP recruits the Dicer complex to Ago2 for microRNA processing and gene silencing. Nature *436*, 740–744.

Choi, Y.J., Lin, C.P., Ho, J.J., He, X., Okada, N., Bu, P., Zhong, Y., Kim, S.Y., Bennett, M.J., Chen, C., et al. (2011). miR-34 miRNAs provide a barrier for somatic cell reprogramming. Nat. Cell Biol. *13*, 1353–1360.

Clarke, M.F., Dick, J.E., Dirks, P.B., Eaves, C.J., Jamieson, C.H., Jones, D.L., Visvader, J., Weissman, I.L., and Wahl, G.M. (2006). Cancer stem cells—perspectives on current status and future directions: AACR Workshop on cancer stem cells. Cancer Res. *66*, 9339–9344.

Clevers, H. (2011). The cancer stem cell: premises, promises and challenges. Nat. Med. *17*, 313–319.

De Vito, C., Riggi, N., Suvà, M.L., Janiszewska, M., Horlbeck, J., Baumer, K., Provero, P., and Stamenkovic, I. (2011). Let-7a is a direct EWS-FLI-1 target implicated in Ewing's sarcoma development. PLoS ONE *6*, e23592.

Esquela-Kerscher, A., Trang, P., Wiggins, J.F., Patrawala, L., Cheng, A., Ford, L., Weidhaas, J.B., Brown, D., Bader, A.G., and Slack, F.J. (2008). The let-7 microRNA reduces tumor growth in mouse models of lung cancer. Cell Cycle *7*, 759–764.

Frank, N.Y., Schatton, T., and Frank, M.H. (2010). The therapeutic promise of the cancer stem cell concept. J. Clin. Invest. *120*, 41–50.

Friedman, J.M., Liang, G., Liu, C.C., Wolff, E.M., Tsai, Y.C., Ye, W., Zhou, X., and Jones, P.A. (2009). The putative tumor suppressor microRNA-101 modulates the cancer epigenome by repressing the polycomb group protein EZH2. Cancer Res. *69*, 2623–2629.

Iliopoulos, D., Hirsch, H.A., Wang, G., and Struhl, K. (2011). Inducible formation of breast cancer stem cells and their dynamic equilibrium with non-stem cancer cells via IL6 secretion. Proc. Natl. Acad. Sci. USA *108*, 1397–1402.

Iorio, M.V., Ferracin, M., Liu, C.G., Veronese, A., Spizzo, R., Sabbioni, S., Magri, E., Pedriali, M., Fabbri, M., Campiglio, M., et al. (2005). MicroRNA gene expression deregulation in human breast cancer. Cancer Res. *65*, 7065–7070.

Jiang, X., Gwye, Y., Russell, D., Cao, C., Douglas, D., Hung, L., Kovar, H., Triche, T.J., and Lawlor, E.R. (2010). CD133 expression in chemo-resistant Ewing sarcoma cells. BMC Cancer *10*, 116.

Kim, H.H., Kuwano, Y., Srikantan, S., Lee, E.K., Martindale, J.L., and Gorospe, M. (2009). HuR recruits let-7/RISC to repress c-Myc expression. Genes Dev. *23*, 1743–1748.

Kim, J., Woo, A.J., Chu, J., Snow, J.W., Fujiwara, Y., Kim, C.G., Cantor, A.B., and Orkin, S.H. (2010). A Myc network accounts for similarities between embryonic stem and cancer cell transcription programs. Cell *143*, 313–324.

Kumar, M.S., Lu, J., Mercer, K.L., Golub, T.R., and Jacks, T. (2007). Impaired microRNA processing enhances cellular transformation and tumorigenesis. Nat. Genet. *39*, 673–677.

Kumar, M.S., Pester, R.E., Chen, C.Y., Lane, K., Chin, C., Lu, J., Kirsch, D.G., Golub, T.R., and Jacks, T. (2009). Dicer1 functions as a haploinsufficient tumor suppressor. Genes Dev. *23*, 2700–2704.

Liu, C., Kelnar, K., Liu, B., Chen, X., Calhoun-Davis, T., Li, H., Patrawala, L., Yan, H., Jeter, C., Honorio, S., et al. (2011). The microRNA miR-34a inhibits prostate cancer stem cells and metastasis by directly repressing CD44. Nat. Med. *17*, 211–215.

Liu, Y., Clem, B., Zuba-Surma, E.K., El-Naggar, S., Telang, S., Jenson, A.B., Wang, Y., Shao, H., Ratajczak, M.Z., Chesney, J., and Dean, D.C. (2009). Mouse fibroblasts lacking RB1 function form spheres and undergo reprogramming to a cancer stem cell phenotype. Cell Stem Cell *4*, 336–347.

Ma, L., Reinhardt, F., Pan, E., Soutschek, J., Bhat, B., Marcusson, E.G., Teruya-Feldstein, J., Bell, G.W., and Weinberg, R.A. (2010a). Therapeutic silencing of miR-10b inhibits metastasis in a mouse mammary tumor model. Nat. Biotechnol. *28*, 341–347.

Ma, S., Tang, K.H., Chan, Y.P., Lee, T.K., Kwan, P.S., Castilho, A., Ng, I., Man, K., Wong, N., To, K.F., et al. (2010b). miR-130b Promotes CD133(+) liver tumor-initiating cell growth and self-renewal via tumor protein 53-induced nuclear protein 1. Cell Stem Cell *7*, 694–707.

Marión, R.M., Strati, K., Li, H., Murga, M., Blanco, R., Ortega, S., Fernandez-Capetillo, O., Serrano, M., and Blasco, M.A. (2009). A p53-mediated DNA damage response limits reprogramming to ensure iPS cell genomic integrity. Nature *460*, 1149–1153.

Melo, S.A., and Esteller, M. (2011). Dysregulation of microRNAs in cancer: playing with fire. FEBS Lett. *585*, 2087–2099.

Melo, S.A., Ropero, S., Moutinho, C., Aaltonen, L.A., Yamamoto, H., Calin, G.A., Rossi, S., Fernandez, A.F., Carneiro, F., Oliveira, C., et al. (2009). A TARBP2 mutation in human cancer impairs microRNA processing and DICER1 function. Nat. Genet. *41*, 365–370.

Melo, S.A., Villanueva, A., Moutinho, C., Davalos, V., Spizzo, R., Ivan, C., Rossi, S., Setien, F., Casanovas, O., Simo-Riudalbas, L., et al. (2011). Small molecule enoxacin is a cancer-specific growth inhibitor that acts by enhancing TAR RNA-binding protein 2-mediated microRNA processing. Proc. Natl. Acad. Sci. USA *108*, 4394–4399.

Nakatani, F., Ferracin, M., Manara, M.C., Ventura, S., Del Monaco, V., Ferrari, S., Alberghini, M., Grilli, A., Knuutila, S., Schaefer, K.L., et al. (2012). miR-34a predicts survival of Ewing's sarcoma patients and directly influences cell chemosensitivity and malignancy. J. Pathol. *226*, 796–805.

Newman, M.A., and Hammond, S.M. (2010). Emerging paradigms of regulated microRNA processing. Genes Dev. *24*, 1086–1092.

Piskounova, E., Polytarchou, C., Thornton, J.E., LaPierre, R.J., Pothoulakis, C., Hagan, J.P., Iliopoulos, D., and Gregory, R.I. (2011). Lin28A and Lin28B inhibit let-7 microRNA biogenesis by distinct mechanisms. Cell *147*, 1066–1079.

Riggi, N., Cironi, L., Provero, P., Suvà, M.L., Kaloulis, K., Garcia-Echeverria, C., Hoffmann, F., Trumpp, A., and Stamenkovic, I. (2005). Development of Ewing's sarcoma from primary bone marrow-derived mesenchymal progenitor cells. Cancer Res. *65*, 11459–11468.

Riggi, N., Cironi, L., Suvà, M.L., and Stamenkovic, I. (2007). Sarcomas: genetics, signalling, and cellular origins. Part 1: The fellowship of TET. J. Pathol. *213*, 4–20.

Riggi, N., Suvà, M.L., Suvà, D., Cironi, L., Provero, P., Tercier, S., Joseph, J.M., Stehle, J.C., Baumer, K., Kindler, V., and Stamenkovic, I. (2008). EWS-FLI-1 expression triggers a Ewing's sarcoma initiation program in primary human mesenchymal stem cells. Cancer Res. *68*, 2176–2185.

Riggi, N., Suvà, M.L., De Vito, C., Provero, P., Stehle, J.C., Baumer, K., Cironi, L., Janiszewska, M., Petricevic, T., Suvà, D., et al. (2010). EWS-FLI-1 modulates miRNA145 and SOX2 expression to initiate mesenchymal stem cell reprogramming toward Ewing sarcoma cancer stem cells. Genes Dev. *24*, 916–932.

Sander, S., Bullinger, L., Klapproth, K., Fiedler, K., Kestler, H.A., Barth, T.F., Möller, P., Stilgenbauer, S., Pollack, J.R., and Wirth, T. (2008). MYC stimulates EZH2 expression by repression of its negative regulator miR-26a. Blood *112*, 4202–4212.

Schepeler, T., Reinert, J.T., Ostenfeld, M.S., Christensen, L.L., Silahtaroglu, A.N., Dyrskjøt, L., Wiuf, C., Sørensen, F.J., Kruhøffer, M., Laurberg, S., et al. (2008). Diagnostic and prognostic microRNAs in stage II colon cancer. Cancer Res. *68*, 6416–6424.

Shan, G., Li, Y., Zhang, J., Li, W., Szulwach, K.E., Duan, R., Faghihi, M.A., Khalil, A.M., Lu, L., Paroo, Z., et al. (2008). A small molecule enhances RNA interference and promotes microRNA processing. Nat. Biotechnol. *26*, 933–940.

Shimono, Y., Zabala, M., Cho, R.W., Lobo, N., Dalerba, P., Qian, D., Diehn, M., Liu, H., Panula, S.P., Chiao, E., et al. (2009). Downregulation of miRNA-200c links breast cancer stem cells with normal stem cells. Cell *138*, 592–603.

Su, H., Yang, J.R., Xu, T., Huang, J., Xu, L., Yuan, Y., and Zhuang, S.M. (2009). MicroRNA-101, down-regulated in hepatocellular carcinoma, promotes apoptosis and suppresses tumorigenicity. Cancer Res. *69*, 1135–1142.

Suvà, M.L., Riggi, N., Stehle, J.C., Baumer, K., Tercier, S., Joseph, J.M., Suvà, D., Clément, V., Provero, P., Cironi, L., et al. (2009). Identification of cancer stem cells in Ewing's sarcoma. Cancer Res. *69*, 1776–1781.

Tan, J., Yang, X., Zhuang, L., Jiang, X., Chen, W., Lee, P.L., Karuturi, R.K., Tan, P.B., Liu, E.T., and Yu, Q. (2007). Pharmacologic disruption of Polycomb-repressive complex 2-mediated gene repression selectively induces apoptosis in cancer cells. Genes Dev. *21*, 1050–1063.

Tong, A.W., and Nemunaitis, J. (2008). Modulation of miRNA activity in human cancer: a new paradigm for cancer gene therapy? Cancer Gene Ther. *15*, 341–355.

Trang, P., Medina, P.P., Wiggins, J.F., Ruffino, L., Kelnar, K., Omotola, M., Homer, R., Brown, D., Bader, A.G., Weidhaas, J.B., and Slack, F.J. (2010). Regression of murine lung tumors by the let-7 microRNA. Oncogene *29*, 1580–1587.

Varambally, S., Cao, Q., Mani, R.S., Shankar, S., Wang, X., Ateeq, B., Laxman, B., Cao, X., Jing, X., Ramnarayanan, K., et al. (2008). Genomic loss of microRNA-101 leads to overexpression of histone methyltransferase EZH2 in cancer. Science *322*, 1695–1699.

Ventura, A., and Jacks, T. (2009). MicroRNAs and cancer: short RNAs go a long way. Cell *136*, 586–591.

Visvader, J.E. (2011). Cells of origin in cancer. Nature *469*, 314–322.

Viswanathan, S.R., Daley, G.Q., and Gregory, R.I. (2008). Selective blockade of microRNA processing by Lin28. Science *320*, 97–100.

Wiggins, J.F., Ruffino, L., Kelnar, K., Omotola, M., Patrawala, L., Brown, D., and Bader, A.G. (2010). Development of a lung cancer therapeutic based on the tumor suppressor microRNA-34. Cancer Res. *70*, 5923–5930.

Wilson, K.D., Venkatasubrahmanyam, S., Jia, F., Sun, N., Butte, A.J., and Wu, J.C. (2009). MicroRNA profiling of human-induced pluripotent stem cells. Stem Cells Dev. *18*, 749–758.

Winter, J., Jung, S., Keller, S., Gregory, R.I., and Diederichs, S. (2009). Many roads to maturity: microRNA biogenesis pathways and their regulation. Nat. Cell Biol. *11*, 228–234.

Wong, D.J., Liu, H., Ridky, T.W., Cassarino, D., Segal, E., and Chang, H.Y. (2008). Module map of stem cell genes guides creation of epithelial cancer stem cells. Cell Stem Cell *2*, 333–344.

Xu, N., Papagiannakopoulos, T., Pan, G., Thomson, J.A., and Kosik, K.S. (2009). MicroRNA-145 regulates OCT4, SOX2, and KLF4 and represses pluripotency in human embryonic stem cells. Cell *137*, 647–658.

Yang, J.S., Maurin, T., Robine, N., Rasmussen, K.D., Jeffrey, K.L., Chandwani, R., Papapetrou, E.P., Sadelain, M., O'Carroll, D., and Lai, E.C. (2010). Conserved vertebrate mir-451 provides a platform for Dicer-independent, Ago2-mediated microRNA biogenesis. Proc. Natl. Acad. Sci. USA *107*, 15163–15168.

Yu, F., Yao, H., Zhu, P., Zhang, X., Pan, Q., Gong, C., Huang, Y., Hu, X., Su, F., Lieberman, J., and Song, E. (2007). let-7 regulates self renewal and tumorigenicity of breast cancer cells. Cell *131*, 1109–1123.